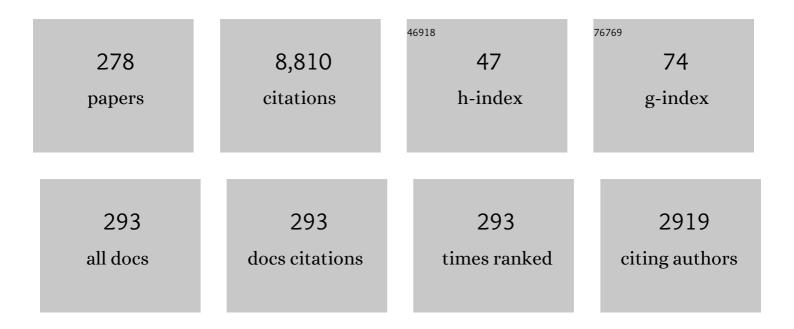
Stephen E Milan

List of Publications by Year in descending order

Source: https://exaly.com/author-pdf/24409/publications.pdf Version: 2024-02-01



STEDHEN F MILAN

#	Article	IF	CITATIONS
1	A decade of the Super Dual Auroral Radar Network (SuperDARN): scientific achievements, new techniques and future directions. Surveys in Geophysics, 2007, 28, 33-109.	2.1	554
2	Variations in the polar cap area during two substorm cycles. Annales Geophysicae, 2003, 21, 1121-1140.	0.6	173
3	Magnetic flux transport in the Dungey cycle: A survey of dayside and nightside reconnection rates. Journal of Geophysical Research, 2007, 112, n/a-n/a.	3.3	165
4	Reconnection in a rotation-dominated magnetosphere and its relation to Saturn's auroral dynamics. Journal of Geophysical Research, 2005, 110, .	3.3	151
5	Convection and auroral response to a southward turning of the IMF: Polar UVI, CUTLASS, and IMAGE signatures of transient magnetic flux transfer at the magnetopause. Journal of Geophysical Research, 2000, 105, 15741-15755.	3.3	150
6	Initial backscatter occurrence statistics from the CUTLASS HF radars. Annales Geophysicae, 1997, 15, 703-718.	0.6	141
7	Relationship between interplanetary parameters and the magnetopause reconnection rate quantified from observations of the expanding polar cap. Journal of Geophysical Research, 2012, 117, .	3.3	118
8	Interplanetary magnetic field at â^1⁄49 AU during the declining phase of the solar cycle and its implications for Saturn's magnetospheric dynamics. Journal of Geophysical Research, 2004, 109, .	3.3	114
9	Review of the accomplishments of mid-latitude Super Dual Auroral Radar Network (SuperDARN) HF radars. Progress in Earth and Planetary Science, 2019, 6, .	1.1	114
10	Overview of Solar Wind–Magnetosphere–Ionosphere–Atmosphere Coupling and the Generation of Magnetospheric Currents. Space Science Reviews, 2017, 206, 547-573.	3.7	105
11	Dayside convection and auroral morphology during an interval of northward interplanetary magnetic field. Annales Geophysicae, 2000, 18, 436-444.	0.6	94
12	CUTLASS Finland radar observations of the ionospheric signatures of flux transfer events and the resulting plasma flows. Annales Geophysicae, 1998, 16, 1411-1422.	0.6	93
13	Open flux estimates in Saturn's magnetosphere during the January 2004 Cassini-HST campaign, and implications for reconnection rates. Journal of Geophysical Research, 2005, 110, .	3.3	92
14	How the IMF <i>B</i> _{<i>y</i>} induces a <i>B</i> _{<i>y</i>} component in the closed magnetosphere and how it leads to asymmetric currents and convection patterns in the two hemispheres. Journal of Geophysical Research: Space Physics, 2015, 120, 9368-9384.	0.8	90
15	Pumping out the atmosphere of Mars through solar wind pressure pulses. Geophysical Research Letters, 2010, 37, .	1.5	88
16	Meridian-scanning photometer, coherent HF radar, and magnetometer observations of the cusp: a case study. Annales Geophysicae, 1999, 17, 159-172.	0.6	87
17	Interplanetary coronal mass ejection observed at STEREOâ€A, Mars, comet 67P/Churyumovâ€Gerasimenko, Saturn, and New Horizons en route to Pluto: Comparison of its Forbush decreases at 1.4, 3.1, and 9.9ÂAU. Journal of Geophysical Research: Space Physics, 2017, 122, 7865-7890.	0.8	87
18	Response of the magnetotail to changes in the open flux content of the magnetosphere. Journal of Geophysical Research, 2004, 109, .	3.3	83

#	Article	IF	CITATIONS
19	Formation and motion of a transpolar arc in response to dayside and nightside reconnection. Journal of Geophysical Research, 2005, 110, .	3.3	83
20	Polarization and phase of planetaryâ€period magnetic field oscillations on highâ€latitude field lines in Saturn's magnetosphere. Journal of Geophysical Research, 2009, 114, .	3.3	83
21	Influences on the radius of the auroral oval. Annales Geophysicae, 2009, 27, 2913-2924.	0.6	82
22	North–South Asymmetries in Earth's Magnetic Field. Space Science Reviews, 2017, 206, 225-257.	3.7	81
23	Interferometric evidence for the observation of ground backscatter originating behind the CUTLASS coherent HF radars. Annales Geophysicae, 1997, 15, 29-39.	0.6	76
24	Seasonal and diurnal variations in AMPERE observations of the Birkeland currents compared to modeled results. Journal of Geophysical Research: Space Physics, 2016, 121, 4027-4040.	0.8	76
25	First simultaneous observations of flux transfer events at the high-latitude magnetopause by the Cluster spacecraft and pulsed radar signatures in the conjugate ionosphere by the CUTLASS and EISCAT radars. Annales Geophysicae, 2001, 19, 1491-1508.	0.6	76
26	Dynamics of the region 1 Birkeland current oval derived from the Active Magnetosphere and Planetary Electrodynamics Response Experiment (AMPERE). Journal of Geophysical Research, 2012, 117, .	3.3	75
27	Stereo CUTLASS - A new capability for the SuperDARN HF radars. Annales Geophysicae, 2004, 22, 459-473.	0.6	74
28	Response of the expanding/contracting polar cap to weak and strong solar wind driving: Implications for substorm onset. Journal of Geophysical Research, 2008, 113, .	3.3	74
29	A superposed epoch analysis of auroral evolution during substorm growth, onset and recovery: open magnetic flux control of substorm intensity. Annales Geophysicae, 2009, 27, 659-668.	0.6	72
30	Dayside and nightside reconnection rates inferred from IMAGE FUV and Super Dual Auroral Radar Network data. Journal of Geophysical Research, 2006, 111, .	3.3	71
31	Bifurcations of the main auroral ring at Saturn: ionospheric signatures of consecutive reconnection events at the magnetopause. Journal of Geophysical Research, 2011, 116, n/a-n/a.	3.3	69
32	Generation region of pulsating aurora obtained simultaneously by the FAST satellite and a Syowa-Iceland conjugate pair of observatories. Journal of Geophysical Research, 2004, 109, .	3.3	67
33	The IMF dependence of the local time of transpolar arcs: Implications for formation mechanism. Journal of Geophysical Research, 2012, 117, .	3.3	67
34	Defining and resolving current systems in geospace. Annales Geophysicae, 2015, 33, 1369-1402.	0.6	66
35	Simultaneous observations of the cusp in optical, DMSP and HF radar data. Geophysical Research Letters, 1997, 24, 2251-2254.	1.5	60
36	The azimuthal extent of three flux transfer events. Annales Geophysicae, 2008, 26, 2353-2369.	0.6	60

#	Article	IF	CITATIONS
37	Both solar windâ€magnetosphere coupling and ring current intensity control of the size of the auroral oval. Geophysical Research Letters, 2009, 36, .	1.5	60
38	The auroral and ionospheric flow signatures of dual lobe reconnection. Annales Geophysicae, 2006, 24, 3115-3129.	0.6	59
39	A survey of magnetopause FTEs and associated flow bursts in the polar ionosphere. Annales Geophysicae, 2000, 18, 416-435.	0.6	58
40	HF radar polar patch formation revisited: summer and winter variations in dayside plasma structuring. Annales Geophysicae, 2002, 20, 487-499.	0.6	58
41	The magnitudes of the regions 1 and 2 Birkeland currents observed by AMPERE and their role in solar windâ€magnetosphereâ€ionosphere coupling. Journal of Geophysical Research: Space Physics, 2014, 119, 9804-9815.	0.8	56
42	Multi-instrument mapping of the small-scale flow dynamics related to a cusp auroral transient. Annales Geophysicae, 2005, 23, 2657-2670.	0.6	54
43	Geomagnetic storms over the last solar cycle: A superposed epoch analysis. Journal of Geophysical Research, 2011, 116, n/a-n/a.	3.3	54
44	Stellar wind–magnetosphere interaction at exoplanets: computations of auroral radio powers. Monthly Notices of the Royal Astronomical Society, 2016, 461, 2353-2366.	1.6	54
45	Statistical study of high-latitude plasma flow during magnetospheric substorms. Annales Geophysicae, 2004, 22, 3607-3624.	0.6	53
46	Superposed epoch analysis of the ionospheric convection evolution during substorms: onset latitude dependence. Annales Geophysicae, 2009, 27, 591-600.	0.6	52
47	Temporal and spatial dynamics of the regions 1 and 2 Birkeland currents during substorms. Journal of Geophysical Research: Space Physics, 2013, 118, 3007-3016.	0.8	52
48	Interplanetary magnetic field control of Saturn's polar cusp aurora. Annales Geophysicae, 2005, 23, 1405-1431.	0.6	51
49	A superposed epoch analysis of the regions 1 and 2 Birkeland currents observed by AMPERE during substorms. Journal of Geophysical Research: Space Physics, 2014, 119, 9834-9846.	0.8	48
50	On the use of IMAGE FUV for estimating the latitude of the open/closed magnetic field line boundary in the ionosphere. Annales Geophysicae, 2008, 26, 2759-2769.	0.6	48
51	Coordinated Cluster/Double Star observations of dayside reconnection signatures. Annales Geophysicae, 2005, 23, 2867-2875.	0.6	47
52	Comment on "Jupiter: A fundamentally different magnetospheric interaction with the solar wind―by D. J. McComas and F. Bagenal. Geophysical Research Letters, 2008, 35, .	1.5	46
53	Direct observation of closed magnetic flux trapped in the high-latitude magnetosphere. Science, 2014, 346, 1506-1510.	6.0	46
54	On the generation of cusp HF backscatter irregularities. Journal of Geophysical Research, 2002, 107, SIA 3-1.	3.3	45

#	Article	IF	CITATIONS
55	Interhemispheric observations of the ionospheric signature of tail reconnection during IMF-northward non-substorm intervals. Annales Geophysicae, 2005, 23, 1763-1770.	0.6	45
56	Average fieldâ€aligned current configuration parameterized by solar wind conditions. Journal of Geophysical Research: Space Physics, 2016, 121, 1294-1307.	0.8	45
57	Motion of flux transfer events: a test of the Cooling model. Annales Geophysicae, 2007, 25, 1669-1690.	0.6	44
58	Characteristics of mediumâ€scale traveling ionospheric disturbances observed near the Antarctic Peninsula by HF radar. Journal of Geophysical Research: Space Physics, 2013, 118, 5830-5841.	0.8	44
59	Coherent HF radar backscatter characteristics associated with auroral forms identified by incoherent radar techniques: A comparison of CUTLASS and EISCAT observations. Journal of Geophysical Research, 1999, 104, 22591-22604.	3.3	42
60	A classification of spectral populations observed in HF radar backscatter from the E region auroral electrojets. Annales Geophysicae, 2001, 19, 189-204.	0.6	42
61	Large-Scale Structure and Dynamics of the Magnetotails of Mercury, Earth, Jupiter and Saturn. Space Science Reviews, 2014, 182, 85-154.	3.7	41
62	The dayside auroral zone as a hard target for coherent HF radars. Geophysical Research Letters, 1998, 25, 3717-3720.	1.5	40
63	Dayside and nightside contributions to the cross polar cap potential: placing an upper limit on a viscous-like interaction. Annales Geophysicae, 2004, 22, 3771-3777.	0.6	40
64	Compression of the Earth's magnetotail by interplanetary shocks directly drives transient magnetic flux closure. Geophysical Research Letters, 2006, 33, n/a-n/a.	1.5	40
65	Solar cycle variations in the ionosphere of Mars as seen by multiple Mars Express data sets. Journal of Geophysical Research: Space Physics, 2016, 121, 2547-2568.	0.8	40
66	A comparison of velocity measurements from the CUTLASS Finland radar and the EISCAT UHF system. Annales Geophysicae, 1999, 17, 892-902.	0.6	39
67	Magnetosonic Mach number dependence of the efficiency of reconnection between planetary and interplanetary magnetic fields. Journal of Geophysical Research, 2009, 114, .	3.3	39
68	Coordinated interhemispheric SuperDARN radar observations of the ionospheric response to flux transfer events observed by the Cluster spacecraft at the high-latitude magnetopause. Annales Geophysicae, 2003, 21, 1807-1826.	0.6	39
69	ESR and EISCAT observations of the response of the cusp and cleft to IMF orientation changes. Annales Geophysicae, 2000, 18, 1009-1026.	0.6	38
70	Superposed epoch analysis of the ionospheric convection evolution during substorms: IMF <i>B</i> _{<i>Y</i>} dependence. Journal of Geophysical Research, 2010, 115, .	3.3	38
71	Principal component analysis of Birkeland currents determined by the Active Magnetosphere and Planetary Electrodynamics Response Experiment. Journal of Geophysical Research: Space Physics, 2015, 120, 10,415.	0.8	38
72	A statistical study of the open magnetic flux content of the magnetosphere at the time of substorm onset. Geophysical Research Letters, 2009, 36, .	1.5	37

#	Article	IF	CITATIONS
73	Modeling Birkeland currents in the expanding/contracting polar cap paradigm. Journal of Geophysical Research: Space Physics, 2013, 118, 5532-5542.	0.8	37
74	The influence of IMF clock angle timescales on the morphology of ionospheric convection. Journal of Geophysical Research: Space Physics, 2014, 119, 5861-5876.	0.8	37
75	The impact of sunlight on highâ€latitude equivalent currents. Journal of Geophysical Research: Space Physics, 2016, 121, 2715-2726.	0.8	37
76	Multi-scale observations of magnetotail flux transport during IMF-northward non-substorm intervals. Annales Geophysicae, 2007, 25, 1709-1720.	0.6	36
77	The BepiColombo Mercury Imaging X-Ray Spectrometer: Science Goals, Instrument Performance and Operations. Space Science Reviews, 2020, 216, 1.	3.7	36
78	Interplanetary magnetic field control of fast azimuthal flows in the nightside highâ€latitude ionosphere. Geophysical Research Letters, 2008, 35, .	1.5	35
79	Observed tail current systems associated with bursty bulk flows and auroral streamers during a period of multiple substorms. Annales Geophysicae, 2008, 26, 167-184.	0.6	35
80	On the influence of open magnetic flux on substorm intensity: Ground―and spaceâ€based observations. Journal of Geophysical Research: Space Physics, 2013, 118, 2958-2969.	0.8	35
81	Magnetospheric response and reconfiguration times following IMF <i>B_y</i> reversals. Journal of Geophysical Research: Space Physics, 2017, 122, 417-431.	0.8	35
82	Timescales for the penetration of IMF <i>B</i> _{<i>y</i>} into the Earth's magnetotail. Journal of Geophysical Research: Space Physics, 2017, 122, 579-593.	0.8	35
83	Plasma structure within poleward-moving cusp/cleft auroral transients: EISCAT Svalbard radar observations and an explanation in terms of large local time extent of events. Annales Geophysicae, 2000, 18, 1027-1042.	0.6	34
84	Cusp ion steps, field-aligned currents and poleward moving auroral forms. Journal of Geophysical Research, 2001, 106, 29555-29569.	3.3	34
85	On the factors controlling occurrence of F-region coherent echoes. Annales Geophysicae, 2002, 20, 1385-1397.	0.6	34
86	Remote sensing of the spatial and temporal structure of magnetopause and magnetotail reconnection from the ionosphere. Reviews of Geophysics, 2008, 46, .	9.0	34
87	In situ observations of the effect of a solar wind compression on Saturn's magnetotail. Journal of Geophysical Research, 2010, 115, .	3.3	33
88	Aurora in the Polar Cap: A Review. Space Science Reviews, 2020, 216, 1.	3.7	33
89	Comparative magnetotail flapping: an overview of selected events at Earth, Jupiter and Saturn. Annales Geophysicae, 2013, 31, 817-833.	0.6	32
90	Are steady magnetospheric convection events prolonged substorms?. Journal of Geophysical Research: Space Physics, 2015, 120, 1751-1758.	0.8	32

#	Article	IF	CITATIONS
91	A case study of HF radar spectra and 630.0 nm auroral emission in the pre-midnight sector. Annales Geophysicae, 2001, 19, 327-339.	0.6	31
92	Ionospheric flows relating to transpolar arc formation. Journal of Geophysical Research, 2012, 117, .	3.3	31
93	IMF control of cusp proton emission intensity and dayside convection: implications for component and anti-parallel reconnection. Annales Geophysicae, 2003, 21, 955-982.	0.6	31
94	A simple model of the flux content of the distant magnetotail. Journal of Geophysical Research, 2004, 109, .	3.3	30
95	A superposed epoch analysis of auroral evolution during substorms: Local time of onset region. Journal of Geophysical Research, 2010, 115, .	3.3	30
96	AXIOM: advanced X-ray imaging of the magnetosphere. Experimental Astronomy, 2012, 33, 403-443.	1.6	30
97	Evidence for transient, local ion foreshocks caused by dayside magnetopause reconnection. Annales Geophysicae, 2016, 34, 943-959.	0.6	30
98	Auroral forms and the field-aligned current structure associated with field line resonances. Journal of Geophysical Research, 2001, 106, 25825-25833.	3.3	29
99	Intensity asymmetries in the dusk sector of the poleward auroral oval due to IMF <i>B</i> _{<i>x</i>} . Journal of Geophysical Research: Space Physics, 2014, 119, 9497-9507.	0.8	29
100	Birkeland current effects on highâ€latitude ground magnetic field perturbations. Geophysical Research Letters, 2015, 42, 7248-7254.	1.5	29
101	Dayside Aurora. Space Science Reviews, 2019, 215, 1.	3.7	29
102	The Heppnerâ€Maynard Boundary measured by SuperDARN as a proxy for the latitude of the auroral oval. Journal of Geophysical Research: Space Physics, 2013, 118, 685-697.	0.8	28
103	The statistical difference between bending arcs and regular polar arcs. Journal of Geophysical Research: Space Physics, 2015, 120, 10,443.	0.8	28
104	How Much Flux Does a Flux Transfer Event Transfer?. Journal of Geophysical Research: Space Physics, 2017, 122, 12,310.	0.8	28
105	Combined CUTLASS, EISCAT and ESR observations of ionospheric plasma flows at the onset of an isolated substorm. Annales Geophysicae, 2000, 18, 1073-1087.	0.6	27
106	Simultaneous observations of flux transfer events by THEMIS, Cluster, Double Star, and SuperDARN: Acceleration of FTEs. Journal of Geophysical Research, 2009, 114, .	3.3	27
107	How the IMF <i>B_y</i> Induces a Local <i>B_y</i> Component During Northward IMF <i>B_z</i> and Characteristic Timescales. Journal of Geophysical Research: Space Physics, 2018, 123, 3333-3348.	0.8	27
108	Origin of the Extended Mars Radar Blackout of September 2017. Journal of Geophysical Research: Space Physics, 2019, 124, 4556-4568.	0.8	27

#	Article	IF	CITATIONS
109	Ground-based observations of the auroral zone and polar cap ionospheric responses to dayside transient reconnection. Annales Geophysicae, 2002, 20, 781-794.	0.6	27
110	Substorm correlated absorption on a 3200 km trans-auroral HF propagation path. Annales Geophysicae, 1996, 14, 182-190.	0.6	26
111	Interhemispheric asymmetries in the occurrence of magnetically conjugate sub-auroral polarisation streams. Annales Geophysicae, 2005, 23, 1371-1390.	0.6	26
112	Seasonal and clock angle control of the location of flux transfer event signatures at the magnetopause. Journal of Geophysical Research, 2012, 117, .	3.3	26
113	Do Statistical Models Capture the Dynamics of the Magnetopause During Sudden Magnetospheric Compressions?. Journal of Geophysical Research: Space Physics, 2020, 125, e2019JA027289.	0.8	26
114	Magnetospheric Flux Throughput in the Dungey Cycle: Identification of Convection State During 2010. Journal of Geophysical Research: Space Physics, 2021, 126, e2020JA028437.	0.8	26
115	SuperDARN radar HF propagation and absorption response to the substorm expansion phase. Annales Geophysicae, 2002, 20, 1631-1645.	0.6	25
116	Multi-instrumentation observations of a transpolar arc in the northern hemisphere. Annales Geophysicae, 2008, 26, 201-210.	0.6	25
117	Deriving solar transient characteristics from single spacecraft STEREO/HI elongation variations: a theoretical assessment of the technique. Annales Geophysicae, 2009, 27, 4359-4368.	0.6	25
118	Comparison between SuperDARN flow vectors and equivalent ionospheric currents from ground magnetometer arrays. Journal of Geophysical Research, 2012, 117, .	3.3	25
119	The interaction between transpolar arcs and cusp spots. Geophysical Research Letters, 2015, 42, 9685-9693.	1.5	25
120	The location of the open-closed magnetic field line boundary in the dawn sector auroral ionosphere. Annales Geophysicae, 2004, 22, 3625-3639.	0.6	24
121	Implications of rapid planetary rotation for the Dungey magnetotail of Saturn. Journal of Geophysical Research, 2005, 110, .	3.3	24
122	On the formation of the high-altitude stagnant cusp: Cluster observations. Geophysical Research Letters, 2005, 32, n/a-n/a.	1.5	24
123	Observations of significant flux closure by dual lobe reconnection. Annales Geophysicae, 2007, 25, 1617-1627.	0.6	24
124	Dynamic effects of restoring footpoint symmetry on closed magnetic field lines. Journal of Geophysical Research: Space Physics, 2016, 121, 3963-3977.	0.8	24
125	Mars plasma system response to solar wind disturbances during solar minimum. Journal of Geophysical Research: Space Physics, 2017, 122, 6611-6634.	0.8	24
126	Simultaneous observations at different altitudes of ionospheric backscatter in the eastward electrojet. Annales Geophysicae, 1998, 16, 55-68.	0.6	23

#	Article	IF	CITATIONS
127	Multistage substorm expansion: Auroral dynamics in relation to plasma sheet particle injection, precipitation, and plasma convection. Journal of Geophysical Research, 2002, 107, SMP 4-1.	3.3	23
128	Direct comparison of pulsating aurora observed simultaneously by the FAST satellite and from the ground at Syowa. Geophysical Research Letters, 2002, 29, 37-1.	1.5	23
129	Average auroral configuration parameterized by geomagnetic activity and solar wind conditions. Annales Geophysicae, 2010, 28, 1003-1012.	0.6	23
130	ECLAT Cluster Spacecraft Magnetotail Plasma Region Identifications (2001–2009). Dataset Papers in Science, 2014, 2014, 1-13.	1.0	23
131	Determining the axial direction of highâ€shear flux transfer events: Implications for models of FTE structure. Journal of Geophysical Research, 2012, 117, .	3.3	22
132	Evidence of scale height variations in the Martian ionosphere over the solar cycle. Journal of Geophysical Research: Space Physics, 2015, 120, 10,913.	0.8	22
133	Dayside reconnection under interplanetary magnetic field <i>B</i> _{<i><by< by<="" i=""></by<></i>} â€dominated conditions: The formation and movement of bending arcs. Journal of Geophysical Research: Space Physics, 2015, 120, 2967-2978.	0.8	22
134	On the altitude dependence of the spectral characteristics of decametre-wavelength E region backscatter and the relationship with optical auroral forms. Annales Geophysicae, 2001, 19, 205-217.	0.6	22
135	Post-noon two-minute period pulsating aurora and their relationship to the dayside convection pattern. Annales Geophysicae, 1999, 17, 877-891.	0.6	21
136	Large flow shears around auroral beads at substorm onset. Geophysical Research Letters, 2013, 40, 4987-4991.	1.5	21
137	What controls the local time extent of flux transfer events?. Journal of Geophysical Research: Space Physics, 2016, 121, 1391-1401.	0.8	21
138	Dual‣obe Reconnection and Horseâ€Collar Auroras. Journal of Geophysical Research: Space Physics, 2020, 125, e2020JA028567.	0.8	21
139	An Explicit IMF B Dependence on Solar Windâ€Magnetosphere Coupling. Geophysical Research Letters, 2020, 47, e2019GL086062.	1.5	21
140	HF radar observations of high-aspect angle backscatter from the E-region. Annales Geophysicae, 2004, 22, 829-847.	0.6	20
141	On the location of dayside magnetic reconnection during an interval of duskward oriented IMF. Annales Geophysicae, 2007, 25, 219-238.	0.6	20
142	Comparison of the open-closed field line boundary location inferred using IMAGE-FUV SI12 images and EISCAT radar observations. Annales Geophysicae, 2010, 28, 883-892.	0.6	20
143	The Association of Highâ€Latitude Dayside Aurora With NBZ Fieldâ€Aligned Currents. Journal of Geophysical Research: Space Physics, 2018, 123, 3637-3645.	0.8	20
144	Velocities of auroral coherent echoes at 12 and 144 MHz. Annales Geophysicae, 2002, 20, 1647-1661.	0.6	19

#	Article	IF	CITATIONS
145	Comparison of the openâ€closed separatrix in a global magnetospheric simulation with observations: The role of the ring current. Journal of Geophysical Research, 2010, 115, .	3.3	19
146	Comparative study of largeâ€scale auroral signatures of substorms, steady magnetospheric convection events, and sawtooth events. Journal of Geophysical Research: Space Physics, 2017, 122, 6357-6373.	0.8	19
147	Transpolar arcs observed simultaneously in both hemispheres. Journal of Geophysical Research: Space Physics, 2017, 122, 6107-6120.	0.8	19
148	Seasonal and Temporal Variations of Fieldâ€Aligned Currents and Ground Magnetic Deflections During Substorms. Journal of Geophysical Research: Space Physics, 2018, 123, 2696-2713.	0.8	19
149	Observations of Asymmetries in Ionospheric Return Flow During Different Levels of Geomagnetic Activity. Journal of Geophysical Research: Space Physics, 2018, 123, 4638-4651.	0.8	19
150	Sun et Lumière: Solar Wind-Magnetosphere Coupling as Deduced from Ionospheric Flows and Polar Auroras. Thirty Years of Astronomical Discovery With UKIRT, 2015, , 33-64.	0.3	19
151	Simultaneous observations of magnetopause flux transfer events and of their associated signatures at ionospheric altitudes. Annales Geophysicae, 2004, 22, 2181-2199.	0.6	19
152	Simultaneous in-situ observations of the signatures of dayside reconnection at the high- and low-latitude magnetopause. Annales Geophysicae, 2005, 23, 445-460.	0.6	19
153	The ionospheric signature of transient dayside reconnection and the associated pulsed convection return flow. Annales Geophysicae, 1999, 17, 1166-1171.	0.6	18
154	Winds and tides in the mid-latitude Southern Hemisphere upper mesosphere recorded with the Falkland Islands SuperDARN radar. Annales Geophysicae, 2011, 29, 1985-1996.	0.6	18
155	Statistical comparison of seasonal variations in the GUMICSâ€4 global MHD model ionosphere and measurements. Space Weather, 2014, 12, 582-600.	1.3	18
156	Azimuthal velocity shear within an Earthward fast flow – further evidence for magnetotail untwisting?. Annales Geophysicae, 2015, 33, 245-255.	0.6	18
157	Dayside and nightside magnetic field responses at 780Âkm altitude to dayside reconnection. Journal of Geophysical Research: Space Physics, 2017, 122, 1670-1689.	0.8	18
158	The asymmetric geospace as displayed during the geomagnetic storm on 17ÂAugustÂ2001. Annales Geophysicae, 2018, 36, 1577-1596.	0.6	18
159	An interhemispheric study of the ground magnetic and ionospheric electric fields during the substorm growth phase and expansion phase onset. Journal of Geophysical Research, 1999, 104, 14867-14877.	3.3	17
160	Extended SuperDARN and IMAGE observations for northward IMF: Evidence for dual lobe reconnection. Journal of Geophysical Research, 2008, 113, .	3.3	17
161	Automatically determining the origin direction and propagation mode of high-frequency radar backscatter. Radio Science, 2015, 50, 1225-1245.	0.8	17
162	Substorm Onset Latitude and the Steadiness of Magnetospheric Convection. Journal of Geophysical Research: Space Physics, 2019, 124, 1738-1752.	0.8	17

#	Article	IF	CITATIONS
163	A superposed epoch investigation of the relation between magnetospheric solar wind driving and substorm dynamics with geosynchronous particle injection signatures. Journal of Geophysical Research, 2011, 116, n/a-n/a.	3.3	16
164	The orientation and current density of the magnetotail current sheet: A statistical study of the effect of geomagnetic conditions. Journal of Geophysical Research, 2012, 117, .	3.3	16
165	Interhemispheric Survey of Polar Cap Aurora. Journal of Geophysical Research: Space Physics, 2018, 123, 7283-7306.	0.8	16
166	Hubble Space Telescope Observations of Variations in Ganymede's Oxygen Atmosphere and Aurora. Journal of Geophysical Research: Space Physics, 2018, 123, 3777-3793.	0.8	16
167	A Statistical Survey of the 630.0â€nm Optical Signature of Periodic Auroral Arcs Resulting From Magnetospheric Field Line Resonances. Geophysical Research Letters, 2018, 45, 4648-4655.	1.5	16
168	Timescales of Dayside and Nightside Fieldâ€Aligned Current Response to Changes in Solar Windâ€Magnetosphere Coupling. Journal of Geophysical Research: Space Physics, 2018, 123, 7307-7319.	0.8	16
169	Modeling the observed proton aurora and ionospheric convection responses to changes in the IMF clock angle: 2. Persistence of ionospheric convection. Journal of Geophysical Research, 2006, 111, .	3.3	15
170	Magnetospheric feedback in solar wind energy transfer. Journal of Geophysical Research, 2010, 115, .	3.3	15
171	Solar cycle variations in polar cap area measured by the superDARN radars. Journal of Geophysical Research: Space Physics, 2013, 118, 6188-6196.	0.8	15
172	Thermospheric density perturbations in response to substorms. Journal of Geophysical Research: Space Physics, 2014, 119, 4441-4455.	0.8	15
173	Saturn's elusive nightside polar arc. Geophysical Research Letters, 2014, 41, 6321-6328.	1.5	15
174	Event study combining magnetospheric and ionospheric perspectives of the substorm current wedge modeling. Journal of Geophysical Research: Space Physics, 2014, 119, 9714-9728.	0.8	15
175	CUTLASS HF radar observations of high-velocity E-region echoes. Annales Geophysicae, 2001, 19, 411-424.	0.6	15
176	Multi-frequency observations of E-region HF radar aurora. Annales Geophysicae, 2003, 21, 761-777.	0.6	15
177	Electrodynamics of an omega-band as deduced from optical and magnetometer data. Annales Geophysicae, 2009, 27, 3367-3385.	0.6	15
178	Open magnetic flux and magnetic flux closure during sawtooth events. Geophysical Research Letters, 2008, 35, .	1.5	14
179	Statistical properties of flux closure induced by solar wind dynamic pressure fronts. Journal of Geophysical Research, 2009, 114, .	3.3	14
180	Dynamic subauroral ionospheric electric fields observed by the Falkland Islands radar during the course of a geomagnetic storm. Journal of Geophysical Research, 2011, 116, n/a-n/a.	3.3	14

#	Article	IF	CITATIONS
181	Modulation of the substorm current wedge by bursty bulk flows: 8 September 2002—Revisited. Journal of Geophysical Research: Space Physics, 2016, 121, 4466-4482.	0.8	14
182	Key Ground-Based and Space-Based Assets to Disentangle Magnetic Field Sources in the Earth's Environment. Space Science Reviews, 2017, 206, 123-156.	3.7	14
183	AMPERE polar cap boundaries. Annales Geophysicae, 2020, 38, 481-490.	0.6	14
184	Statistical characteristics of Doppler spectral width as observed by the conjugate SuperDARN radars. Annales Geophysicae, 2002, 20, 1213-1223.	0.6	13
185	D region HF radar echoes associated with energetic particle precipitation and pulsating aurora. Annales Geophysicae, 2008, 26, 1897-1904.	0.6	13
186	Tracking corotating interaction regions from the Sun through to the orbit of Mars using ACE, MEX, VEX, and STEREO. Journal of Geophysical Research, 2011, 116, n/a-n/a.	3.3	13
187	One year in the Earth's magnetosphere: A global MHD simulation and spacecraft measurements. Space Weather, 2016, 14, 351-367.	1.3	13
188	Phase calibration of interferometer arrays at highâ€frequency radars. Radio Science, 2016, 51, 1445-1456.	0.8	13
189	Modeling the magnetospheric Xâ€ray emission from solar wind charge exchange with verification from XMMâ€Newton observations. Journal of Geophysical Research: Space Physics, 2016, 121, 4158-4179.	0.8	13
190	Separation and Quantification of Ionospheric Convection Sources: 2. The Dipole Tilt Angle Influence on Reverse Convection Cells During Northward IMF. Journal of Geophysical Research: Space Physics, 2019, 124, 6182-6194.	0.8	13
191	The Evolution of Longâ€Duration Cusp Spot Emission During Lobe Reconnection With Respect to Fieldâ€Aligned Currents. Journal of Geophysical Research: Space Physics, 2020, 125, e2020JA027922.	0.8	13
192	The Impact of Energetic Particles on the Martian Ionosphere During a Full Solar Cycle of Radar Observations: Radar Blackouts. Journal of Geophysical Research: Space Physics, 2022, 127, .	0.8	13
193	Global-scale observations of ionospheric convection during geomagnetic storms. Journal of Geophysical Research, 2011, 116, n/a-n/a.	3.3	12
194	Storm and substorm effects on magnetotail current sheet motion. Journal of Geophysical Research, 2012, 117, .	3.3	12
195	Testing nowcasts of the ionospheric convection from the expanding and contracting polar cap model. Space Weather, 2017, 15, 623-636.	1.3	12
196	Mixed Azimuthal Scales of Flux Transfer Events. Thirty Years of Astronomical Discovery With UKIRT, 2010, , 389-398.	0.3	12
197	A comparison of satellite scintillation measurements with HF radar backscatter characteristics. Annales Geophysicae, 2005, 23, 3451-3455.	0.6	11
198	Heights of SuperDARN F region echoes estimated from the analysis of HF radio wave propagation. Annales Geophysicae, 2007, 25, 1987-1994.	0.6	11

#	Article	IF	CITATIONS
199	Verification of the GUMICSâ€4 global MHD code using empirical relationships. Journal of Geophysical Research: Space Physics, 2013, 118, 3138-3146.	0.8	11
200	Joule heating hot spot at high latitudes in the afternoon sector. Journal of Geophysical Research: Space Physics, 2016, 121, 7135-7152.	0.8	11
201	Energetic Particle Showers Over Mars from Comet C/2013 A1 Siding Spring. Journal of Geophysical Research: Space Physics, 2018, 123, 8778-8796.	0.8	11
202	A comparison of F-region ion velocity observations from the EISCAT Svalbard and VHF radars with irregularity drift velocity measurements from the CUTLASS Finland HF radar. Annales Geophysicae, 2000, 18, 589-594.	0.6	11
203	Lobe Reconnection and Cuspâ€Aligned Auroral Arcs. Journal of Geophysical Research: Space Physics, 2022, 127, .	0.8	11
204	Electrodynamics of a split-transpolar aurora. Journal of Geophysical Research, 2006, 111, .	3.3	10
205	A Wide Field Auroral Imager (WFAI) for low Earth orbit missions. Annales Geophysicae, 2007, 25, 519-532.	0.6	10
206	Electric field modulation behind pulsating aurora. Journal of Geophysical Research, 2008, 113, .	3.3	10
207	Effects of a solar wind dynamic pressure increase in the magnetosphere and in the ionosphere. Annales Geophysicae, 2010, 28, 1945-1959.	0.6	10
208	A quantitative deconstruction of the morphology of highâ€latitude ionospheric convection. Journal of Geophysical Research, 2012, 117, .	3.3	10
209	Magnetotail magnetic flux monitoring based on simultaneous solar wind and magnetotail observations. Journal of Geophysical Research: Space Physics, 2016, 121, 8821-8839.	0.8	10
210	Observations of Asymmetric Lobe Convection for Weak and Strong Tail Activity. Journal of Geophysical Research: Space Physics, 2019, 124, 9999-10017.	0.8	10
211	Heightâ€Integrated Ionospheric Conductances Parameterized By Interplanetary Magnetic Field and Substorm Phase. Journal of Geophysical Research: Space Physics, 2020, 125, e2020JA028121.	0.8	10
212	A seasonal variation in the convection response to IMF orientation. Geophysical Research Letters, 2001, 28, 471-474.	1.5	9
213	An assessment of the "map-potential" and "beam-swinging" techniques for measuring the ionospheric convection pattern using data from the SuperDARN radars. Annales Geophysicae, 2002, 20, 191-202.	0.6	9
214	Modulation of dayside reconnection during northward interplanetary magnetic field. Journal of Geophysical Research, 2005, 110, .	3.3	9
215	Globalâ€scale observations of ionospheric convection variation in response to sudden increases in the solar wind dynamic pressure. Journal of Geophysical Research, 2012, 117, .	3.3	9
216	Alfvén: magnetosphere—ionosphere connection explorers. Experimental Astronomy, 2012, 33, 445-489.	1.6	9

#	Article	IF	CITATIONS
217	The Influence of IMF Clock Angle on Dayside Flux Transfer Events at Mercury. Geophysical Research Letters, 2017, 44, 10,829.	1.5	9
218	Separation and Quantification of Ionospheric Convection Sources: 1. A New Technique. Journal of Geophysical Research: Space Physics, 2019, 124, 6343-6357.	0.8	9
219	An Improved Estimation of SuperDARN Heppnerâ€Maynard Boundaries Using AMPERE Data. Journal of Geophysical Research: Space Physics, 2020, 125, e2019JA027218.	0.8	9
220	A Ray Tracing Simulation of HF Ionospheric Radar Performance at African Equatorial Latitudes. Radio Science, 2020, 55, e2019RS006936.	0.8	9
221	Average Ionospheric Electric Field Morphologies During Geomagnetic Storm Phases. Journal of Geophysical Research: Space Physics, 2021, 126, e2020JA028512.	0.8	9
222	An inter-hemispheric, statistical study of nightside spectral width distributions from coherent HF scatter radars. Annales Geophysicae, 2002, 20, 1921-1934.	0.6	9
223	Occurrence Statistics of Horse Collar Aurora. Journal of Geophysical Research: Space Physics, 2022, 127, .	0.8	9
224	Investigation of the relationship between optical auroral forms and HF radar E region backscatter. Annales Geophysicae, 2000, 18, 608-617.	0.6	8
225	Flux closure during a substorm observed by Cluster, Double Star, IMAGE FUV, SuperDARN, and Greenland magnetometers. Annales Geophysicae, 2006, 24, 751-767.	0.6	8
226	Asymmetry in the bipolar signatures of flux transfer events. Journal of Geophysical Research, 2010, 115,	3.3	8
227	The spectral characteristics of E-region radar echoes co-located with and adjacent to visual auroral arcs. Annales Geophysicae, 2002, 20, 795-805.	0.6	8
228	Interhemispheric comparison of spectral width boundary as observed by SuperDARN radars. Annales Geophysicae, 2003, 21, 1553-1565.	0.6	8
229	Interplanetary magnetic fieldBydependence of the relative position of the dayside ultraviolet auroral oval and the HF radar cusp. Journal of Geophysical Research, 2001, 106, 29027-29036.	3.3	7
230	High resolution observations of spectral width features associatedwith ULF wave signatures in artificial HF radar backscatter. Annales Geophysicae, 2004, 22, 169-182.	0.6	7
231	Cluster magnetotail observations of a tailward-travelling plasmoid at substorm expansion phase onset and field aligned currents in the plasma sheet boundary layer. Annales Geophysicae, 2005, 23, 3667-3683.	0.6	7
232	A first comparison of irregularity and ion drift velocity measurements in the E-region. Annales Geophysicae, 2006, 24, 2375-2389.	0.6	7
233	Auroral streamers and magnetic flux closure. Geophysical Research Letters, 2007, 34, .	1.5	7
234	Solar Influences on the Return Direction of Highâ€Frequency Radar Backscatter. Radio Science, 2018, 53, 577-597.	0.8	7

#	Article	IF	CITATIONS
235	Bifurcated Region 2 Fieldâ€Aligned Currents Associated With Substorms. Journal of Geophysical Research: Space Physics, 2020, 125, e2019JA027041.	0.8	7
236	Cusp observations during a sequence of fast IMF <l>B_Z</l> reversals. Annales Geophysicae, 2009, 27, 2721-2737.	0.6	6
237	Simultaneous groundâ€satellite observations of mesoâ€scale auroral arc undulations. Journal of Geophysical Research, 2012, 117, .	3.3	6
238	Assessing the Effect of Spacecraft Motion on Single-Spacecraft Solar Wind Tracking Techniques. Solar Physics, 2014, 289, 3935-3947.	1.0	6
239	Corotating Interaction Regions as Seen by the STEREO Heliospheric Imagers 2007 – 2010. Solar Physi 2015, 290, 2291-2309.	cs. 1.0	6
240	Magnetic reconnection during steady magnetospheric convection and other magnetospheric modes. Annales Geophysicae, 2017, 35, 505-524.	0.6	6
241	E-region echo characteristics governed by auroral arc electrodynamics. Annales Geophysicae, 2003, 21, 1567-1575.	0.6	6
242	Polar observations of the time-varying cusp. Journal of Geophysical Research, 2001, 106, 19057-19065.	3.3	5
243	An investigation of the field-aligned currents associated with a large-scale ULF wave using data from CUTLASS and FAST. Annales Geophysicae, 2005, 23, 487-498.	0.6	5
244	Double Star, Cluster, and ground-based observations of magnetic reconnection during an interval of duskward oriented IMF: preliminary results. Annales Geophysicae, 2005, 23, 2903-2907.	0.6	5
245	Review of Ionospheric Effects of Solar Wind Magnetosphere Coupling in the Context of the Expanding Contracting Polar Cap Boundary Model. Space Science Reviews, 2007, 124, 117-130.	3.7	5
246	Plasma irregularities adjacent to auroral patches in the postmidnight sector. Journal of Geophysical Research, 2010, 115, .	3.3	5
247	A new way to study geomagnetic storms. Astronomy and Geophysics, 2011, 52, 4.20-4.23.	0.1	5
248	KuaFu: exploring the Sun-Earth connection. Astronomy and Geophysics, 2012, 53, 4.21-4.24.	0.1	5
249	Traveling ionospheric disturbances in the Weddell Sea Anomaly associated with geomagnetic activity. Journal of Geophysical Research: Space Physics, 2013, 118, 6608-6617.	0.8	5
250	Probing the Magnetic Structure of a Pair of Transpolar Arcs With a Solar Wind Pressure Step. Journal of Geophysical Research: Space Physics, 2020, 125, e2019JA027196.	0.8	5
251	A comparison of optical and coherent HF radar backscatter observations of a post-midnight aurora. Annales Geophysicae, 1997, 15, 1388-1398.	0.6	4
252	Multipulse and double-pulse velocities of Scandinavian Twin Auroral Radar Experiment (STARE) echoes. Radio Science, 2005, 40, n/a-n/a.	0.8	4

#	Article	IF	CITATIONS
253	A Study of Observations of Ionospheric Upwelling Made by the EISCAT Svalbard Radar During the International Polar Year Campaign of 2007. Journal of Geophysical Research: Space Physics, 2018, 123, 2192-2203.	0.8	4
254	Machine Learning Analysis of Jupiter's Farâ€Ultraviolet Auroral Morphology. Journal of Geophysical Research: Space Physics, 2019, 124, 8884-8892.	0.8	4
255	Unusual ionospheric echoes with high velocity and very low spectral width observed by the SuperDARN radars in the polar cap during high geomagnetic activity. Journal of Geophysical Research, 2004, 109, .	3.3	3
256	Concurrent Observations Of Magnetic Reconnection From Cluster, IMAGE and SuperDARN: A Comparison Of Reconnection Rates And Energy Conversion. Journal of Geophysical Research: Space Physics, 2020, 125, e2019JA027264.	0.8	3
257	Exploring solar-terrestrial interactions via multiple imaging observers. Experimental Astronomy, 0, , 1.	1.6	3
258	Planetary Period Oscillations of Saturn's Dayside Equatorial Ionospheric Electron Density Observed on Cassini's Proximal Passes. Journal of Geophysical Research: Space Physics, 2021, 126, e2021JA029332.	0.8	3
259	Review of Ionospheric Effects of Solar Wind Magnetosphere Coupling in the Context of the Expanding Contracting Polar Cap Boundary Model. Space Sciences Series of ISSI, 2007, , 117-130.	0.0	3
260	A multi-instrument approach to mapping the global dayside merging rate. Annales Geophysicae, 2002, 20, 1905-1920.	0.6	2
261	A joint Cluster and ground-based instruments study of two magnetospheric substorm events on 1 September 2002. Annales Geophysicae, 2004, 22, 4217-4228.	0.6	2
262	Whose field line is it anyway?. Astronomy and Geophysics, 2004, 45, 3.36-3.38.	0.1	2
263	Transpolar Arcs: Seasonal Dependence Identified by an Automated Detection Algorithm. Journal of Geophysical Research: Space Physics, 2022, 127, .	0.8	2
264	Statistical Analysis of Bifurcating Region 2 Field-Aligned Currents Using AMPERE. Frontiers in Astronomy and Space Sciences, 2022, 9, .	1.1	2
265	Influence of Offâ€Sunâ€Earth Line Distance on the Accuracy of L1 Solar Wind Monitoring. Journal of Geophysical Research: Space Physics, 2022, 127, .	0.8	2
266	Statistics of the mid-altitude cusp observed by Polar. Geophysical Research Letters, 2002, 29, 5-1-5-4.	1.5	1
267	Looking through the oval window. Astronomy and Geophysics, 2008, 49, 4.16-4.18.	0.1	1
268	A statistical study of the spatial distribution of Coâ€operative UK Twin Located Auroral Sounding System (CUTLASS) backscatter power during EISCAT heater beamâ€sweeping experiments. Journal of Geophysical Research, 2010, 115, .	3.3	1
269	Combining incoherent scatter radar data and IRIâ€2007 to monitor the openâ€closed field line boundary during substorms. Journal of Geophysical Research, 2010, 115, .	3.3	1
270	AXIOM: Advanced Xâ€ray imaging of the magnetosheath. Astronomische Nachrichten, 2012, 333, 388-392.	0.6	1

#	Article	IF	CITATIONS
271	An analysis of magnetic reconnection events and their associated auroral enhancements. Journal of Geophysical Research: Space Physics, 2017, 122, 2922-2935.	0.8	1
272	Key Ground-Based and Space-Based Assets to Disentangle Magnetic Field Sources in the Earth's Environment. Space Sciences Series of ISSI, 2018, , 125-158.	0.0	1
273	Magnetotails throughout the solar system. Astronomy and Geophysics, 2010, 51, 6.28-6.30.	0.1	0
274	Magnetic fields in a flap!. Astronomy and Geophysics, 2011, 52, 4.17-4.19.	0.1	0
275	The changing polar ionosphere: A comparative climatology of solar cycles 23 and 24. , 2015, , .		0
276	North–South Asymmetries in Earth's Magnetic Field. Space Sciences Series of ISSI, 2018, , 231-263.	0.0	0
277	Overview of Solar Wind–Magnetosphere–Ionosphere–Atmosphere Coupling and the Generation of Magnetospheric Currents. Space Sciences Series of ISSI, 2018, , 555-581.	0.0	0
278	Fieldâ€Aligned Current During an Interval of B _{<i>Y</i>} â€Dominated Interplanetaryâ€Field; Modeledâ€ŧoâ€Observed Comparisons. Journal of Geophysical Research: Space Physics, 2021, 126, .	0.8	0